



OPEN ACCESS

EDITED BY

Eric Robert,
UMR7344 Groupe de recherches sur
l'énergétique des milieux ionisés (GREMI),
France

REVIEWED BY

Pradeep Lamichhane,
University of Warwick, United Kingdom
Sohail Mumtaz,
Kwangwoon University, Republic of Korea

*CORRESPONDENCE

Paolo Francesco Ambrico,
✉ paolofrancesco.ambrico@cnr.it
Rita Milvia De Miccolis Angelini,
✉ ritamilvia.demiccolisangelini@uniba.it

†These authors have contributed equally to this work and share last authorship

RECEIVED 12 March 2024

ACCEPTED 09 April 2024

PUBLISHED 06 May 2024

CITATION

Aceto D, Rotondo PR, Porfido C, Bottiglione B, Paciolla C, Terzano R, Minafra A, Ambrico M, Dilecce G, Leoni B, De Miccolis Angelini RM and Ambrico PF (2024), Assessing plasma activated water irrigation effects on tomato seedlings. *Front. Phys.* 12:1399910. doi: 10.3389/fphy.2024.1399910

COPYRIGHT

© 2024 Aceto, Rotondo, Porfido, Bottiglione, Paciolla, Terzano, Minafra, Ambrico, Dilecce, Leoni, De Miccolis Angelini and Ambrico. This is an open-access article distributed under the terms of the [Creative Commons Attribution License \(CC BY\)](https://creativecommons.org/licenses/by/4.0/). The use, distribution or reproduction in other forums is permitted, provided the original author(s) and the copyright owner(s) are credited and that the original publication in this journal is cited, in accordance with accepted academic practice. No use, distribution or reproduction is permitted which does not comply with these terms.

Assessing plasma activated water irrigation effects on tomato seedlings

Domenico Aceto¹, Palma Rosa Rotondo², Carlo Porfido², Benedetta Bottiglione³, Costantino Paciolla³, Roberto Terzano², Angelantonio Minafra⁴, Marianna Ambrico¹, Giorgio Dilecce¹, Beniamino Leoni², Rita Milvia De Miccolis Angelini^{2*†} and Paolo Francesco Ambrico^{1*†}

¹CNR Istituto per la Scienza e Tecnologia dei Plasmi–Sede di Bari–c/o Dipartimento Interateneo di Fisica–Campus Universitario “Ernesto Quagliariello”, Università degli Studi di Bari Aldo Moro, Bari, Italy, ²Dipartimento di Scienze del Suolo, della Pianta e degli Alimenti (Di.S.S.P.A.), Campus Universitario “Ernesto Quagliariello”, Università degli Studi di Bari Aldo Moro, Bari, Italy, ³Dipartimento di Bioscienze, Biotechnologie e Ambiente (DBBA), Campus Universitario “Ernesto Quagliariello”, Università degli Studi di Bari Aldo Moro, Bari, Italy, ⁴CNR Istituto per la Protezione Sostenibile delle Piante–Sede di Bari–c/o Campus Universitario “Ernesto Quagliariello”, Università degli Studi di Bari Aldo Moro, Bari, Italy

Introduction: The study investigates the potential of Plasma Activated Water (PAW) as an innovative irrigation medium to enhance growth and defense responses in tomato seedlings. It explores PAW's utility in both healthy seedlings and those inoculated with *Tomato mottle mosaic virus* (ToMMV).

Methods: PAW, produced through a dielectric barrier volume discharge, serves as a chemical-free alternative to traditional fertilizers. Tomato seedlings were irrigated with PAW or control solutions. The study employs biometric measurements to assess growth and biochemical analysis to evaluate antioxidant levels and pigments. Gene expression analysis was conducted to evaluate the plant response, while the distribution of macro and micronutrients was assessed through micro X-ray fluorescence.

Results and discussion: Results indicate that PAW-irrigated seedlings exhibit significant growth enhancement compared to those receiving conventional fertilization. Increased levels of antioxidant molecules and pigments suggest improved photosynthetic activity and stress tolerance. Gene expression analysis shows up-regulation of defense genes in PAW-treated plants post-viral infection. The up-regulation of defense genes and the restoration of mineral nutrient distribution in PAW-treated, virus-infected plants highlight PAW's role in enhancing plant resilience against pathogens and mitigating nutrient deficiencies. These findings emphasize PAW's potential as a sustainable agricultural solution, promoting plant growth, enhancing defense mechanisms, and reducing biotic stress due to virus infections.

KEYWORDS

PAW, low-temperature-plasma, tomato seedlings, plant growth, gene expression, tomato mottle mosaic virus, micro X-ray fluorescence

1 Introduction

In the last decade, the need for suitable, innovative, and non-chemical strategies for agrifood production and plant protection has given rise to new tools for microbial decontamination, plant resistance induction, and enhancement of growth and nutraceutical properties of products. Low-temperature plasma is proposed as a revolutionary tool in modern agriculture, offering versatile applications that span from seed treatment to soil improvement [1]. This novel approach involves subjecting agricultural systems to non-thermal plasma, generating reactive species such as reactive oxygen species (ROS) and reactive nitrogen species (RNS). These plasma-induced reactive species have shown great potential in influencing various aspects of plant growth, stress response, and overall crop performance [2–4]. However, plasma treatments are mainly confined to the surface of materials, and therefore not able to interact with all plant tissues. Thus, different strategies are required for applications, such as the production and usage of plasma-activated media.

In conjunction with the advancements in low-temperature plasma applications, Plasma Activated Water (PAW) has emerged as a cutting-edge and transformative tool in modern agriculture, offering promising potential to enhance crop productivity and address various challenges faced by the industry. This novel approach involves subjecting water to non-thermal plasma exposing it to ROS and RNS [5] and inducing changes in the physicochemical properties of the liquid. These changes can be tailored for different applications [6,7]. Reactive species in PAW impart beneficial effects on plants inducing physiological and biochemical changes with positive effects on growth and stress tolerance [6]. Thus, PAW can be used for watering crops, soaking seeds, and spraying on foliage, being a sustainable and environmentally friendly alternative to traditional chemical fertilizers and pesticides. Recent research on PAW has shown its potential in agriculture. Studies have found that PAW can enhance seed germination, plant growth, and yield across various crops like wheat, cucumber, and tomato [8,9]. It also improves photosynthetic efficiency, and antioxidant enzyme activities [10], and induces self-defense mechanisms in plants [11,12]. However, further research is needed to fully harness its potential.

In this investigation, we studied the potential of PAW to promote the growth of tomato plants under both normal and virus-induced stress conditions, caused by *Tomato mottle mosaic virus* (ToMMV) infection. This dual-pronged approach allowed us to unravel the biological and physiological mechanisms underlying the multifaceted effects of PAW on the growth of both healthy and virus-inoculated plants.

In the examination of healthy plants, our study employed a comprehensive set of parameters to assess the impact of PAW. We closely monitored the growth of the tomato plants, by measuring parameters such as stem length, diameter and leaf area, and the influence of PAW on key components of the plant's antioxidant defense system, including ascorbate, glutathione, chlorophylls, and carotenoids content. Additionally, the gene expression of four different defense-related genes [phenylalanine ammonia-lyase (PAL), pathogenesis-related protein 1 (PR-1), lipoxygenase (LOX), and catalase (CAT)] was analyzed to explore tomato plant responses after PAW irrigation and ToMMV inoculation. Expanding our focus to plants subjected to ToMMV-induced stress, we implemented a comparative analysis employing micro X-ray fluorescence (μ -XRF) spectroscopy to visualize the changes in the distribution of micro and macro-nutrients in the plant leaves,

unveiling insights into the nuanced responses mechanisms of virus-inoculated plants to PAW treatment.

2 Materials and methods

2.1 Plasma activated water production

The plasma reactor employed in this study (Figure 1B) operates on an AC voltage with a frequency of 13 kHz, modulated by a square pulse at a 500 Hz repetition rate with a 38% duty cycle. A schematic of the plasma reactor is shown in Figure 1A. A glass pot is used as the water reservoir and reaction chamber. The pot is closed at the top by a plexiglass cover with holes to house the high-voltage electrodes and the gas inlet tube. The six high-voltage electrodes consist of metal pins enclosed in quartz sleeves. At the bottom of the pot, on its outer face, a copper tape shaped like a hexagon, positioned to have its vertices lining up with the HV electrodes, serves as the grounded electrode. Thus, two dielectric barriers are interposed between the electrodes. When the chamber is filled up with double-distilled water, the liquid itself acts as another dielectric layer and establishes a discharge gap of 5 mm. The double dielectric configuration enhances the reproducibility of the pulsed discharge, ensuring stable plasma activation conditions. A controlled airflow of 2 standard liters per minute (slm) is insufflated directly into the water, providing a complete replacement of the gas in the whole vessel in less than a minute and increasing the water vapor content in the gas mixture, possibly enhancing hydrogen peroxide formation. However, due to the presence of cool walls, the evaporation induced by gas flow and temperature does not reduce the total water volume as vapor condenses on the outer wall of the vessel. Each treatment involves subjecting 500 mL of double-distilled water (RPE Carlo Erba Reagents) to this dynamic process, with continuous stirring to guarantee homogenous exposure. The treatment protocol consists of four 15-min steps, allowing for meticulous control and modulation of the plasma activation parameters. A picture of the setup during the water treatment is reported in Figure 1B.

The discharge voltage-charge and voltage-current characteristics were recorded using a Keysight InfiniiVision MSOX6004A with a bandwidth of 1 GHz and a sampling rate of up to 20 GS/s. To measure the applied voltage, a Tektronix P6015A high voltage probe with a ratio of 1,000:1 at 1 M Ω , a bandwidth of 25 MHz, and a rise time of 4.7 ns was employed. The current was measured using a Magnelab CT-c1.0 Rogowski coil with a rise time of 0.7 ns attached to the ground cable. Additionally, charge measurements were obtained by inserting a 2.4 nF high-voltage capacitor between the induction electrode and the ground. The energy was measured from charge-voltage Lissajous characteristics by integrating them.

The optical diagnostic was performed through a slit in the glass vessel (1.5 mm \times 30 mm) closed by a quartz window. The Plasma Induced Emission (PIE) was collected by an optical fiber designed to adapt to the monochromator slit with a maximum size of 3 mm in width and 5 mm in height. A 30 cm spectrometer (Acton Spectra Pro 2,300) was employed for spectral resolution, featuring a multiple-grating turret (300/600/1200 grooves \times mm $^{-1}$, blazed at 300 nm) and a Princeton Instruments PI-MAX4 1024i CCD (1024 \times 1024 pixel sensor, pixel size 12.8 μ m, active area 13.1 \times 13.1 mm 2). Each CCD image covers a spectral range of approximately 144/65/30 nm for the three gratings. The emission

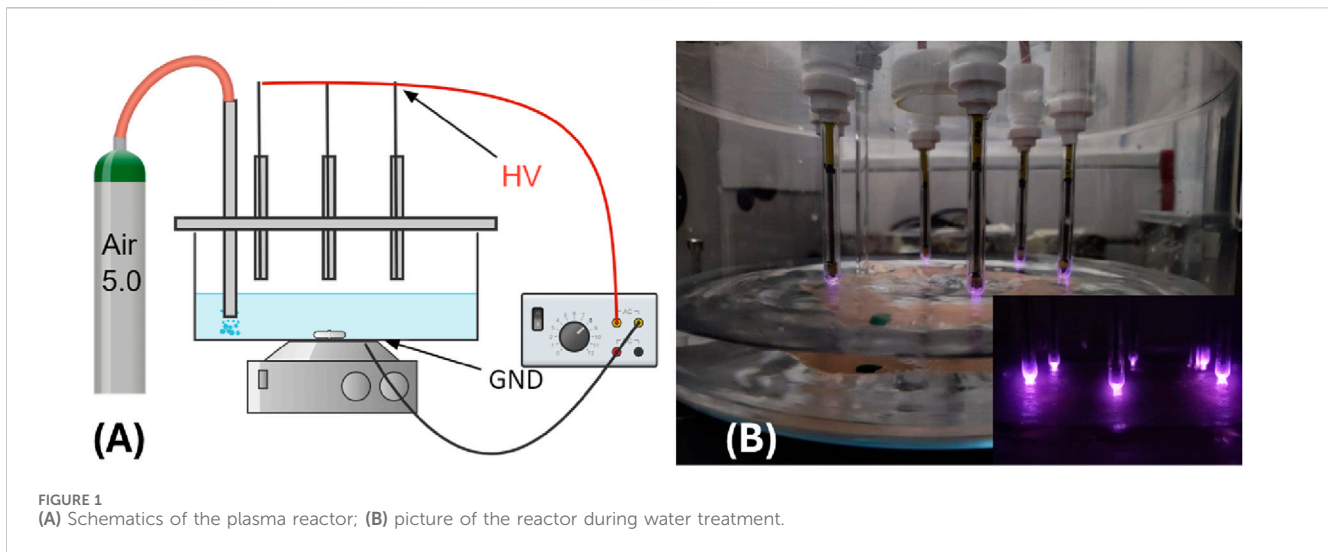


FIGURE 1
(A) Schematics of the plasma reactor; (B) picture of the reactor during water treatment.

spectra intensities, detected by the ICCD (Intensified CCD) detector, undergo spectral and intensity correction through calibration and Halogen lamps. These captured spectra are time-resolved with a 50 μ s gate at the start of each high-voltage (HV) half cycle.

2.2 Quantification of reactive nitrogen and oxygen species (RONS) produced in PAW

The PAW was characterized in its chemical composition in terms of the active species identified in the literature as responsible for its biological effects: nitrite and nitrate ions and hydrogen peroxide content. The concentration of the different reactive species was measured using a multiparametric photometer Aqualytic AL400 and Cell Test Lovibond® Water Testing (Tintometer Inc., Germany), according to the manufacturer's instructions for quantification of nitrate ions (Vario Nitra protocol X 535,580, quantification range 0–30 mg L⁻¹), nitrite ions (protocol 512310BT, range 0.01–0.5 mg L⁻¹) and hydrogen peroxide (protocol 512381BT, range 0.03–3 mg L⁻¹). Due to the concentration of active species being higher than the quantification range, in most cases prior to measuring it was necessary to dilute the PAW with the same double-distilled water used to produce it. When the sample was diluted, the results of the tests were multiplied by the corresponding dilution factor.

The pH and oxidation-reduction potential (ORP) values were measured with a HANNA Instruments (USA) pH-meter model HI98191 equipped with a HI72911 pH probe and a HI3131 ORP probe.

2.3 Plant growth and irrigation with PAW

Seeds of tomato (*Solanum lycopersicum* L.) cv. Regina were sown, and the seedlings were then transplanted in a commercial peat moss substrate (BRILL Typical 3, Germany) at the “two true-leaves” stage. Pots (9 × 14 × 5 cm³) were kept in a thermo-conditioned glasshouse box at 25°C ± 2°C and exposed to Osram L36W Cool White lamps with an 18 h photoperiod.

After the transplant, the seedlings were daily irrigated with 5 mL of the appropriate solution according to the irrigation treatment reported

in Table 1. Two positive control solutions, consisting of 1 g L⁻¹ ammonium nitrate (YaraTera AMNITRA, Norway), and 0.5 g L⁻¹ of the commercial fertilizer (Nitrophoska® Special 12–12–17, NPK-based, EuroChem, Switzerland) were used. Double-distilled water (RPE Carlo Erba Reagents, Italy) was used as the negative control.

Three seedlings per pot represented a single biological replicate. All treatments were performed in three replicates per analysis and the experiments were repeated twice.

2.4 Biometric measurements

The stem length, diameter, and leaf surface area were measured 21 days after the first irrigation time. Biometric measurements were performed by collecting RGB images through a Digital reflex camera with a 50 mm objective (Nikon D5300) of the entire plant and the last three apical leaves of each plant branch. Images were then calibrated with respect to a target of known dimension to extract the pixel/cm conversion constant. The leaf area and stem length were then processed via the freely available Digimizer Image Analysis Software [13]. A total of 18 plants per treatment were analyzed.

2.5 Determination of chlorophyll and carotenoid content, and ascorbate and glutathione pools

The chlorophyll and carotenoid content was determined according to Lichtenthaler [14] with some modifications. Samples of uninoculated seedlings (NTDDW, WNPK, WAN, PAW) were irrigated for 21 days after transplant and subsequently analyzed. In detail, 0.5 g of the aerial part of the seedling were ground with 8 mL of absolute acetone and centrifuged at 20,000 × g for 15 min. The absorbance of the supernatant (total filtrate volume in mL) was spectrophotometrically measured (Beckman DU-800 UV/Vis spectrophotometer, Beckman Coulter, Inc., USA) at 645 nm for chlorophyll *a*, 662 nm for chlorophyll *b*, and 470 nm for carotenoids. Chlorophyll (Chl *a*, *b*, and *a+b*) and carotenoids (Car) contents were calculated using the following equations:

TABLE 1 Summary of the plant growth conditions explored.

Treatment conditions	Sample code
Plants irrigated with double-distilled water	NTDDW
Plants irrigated with tap water added with standard fertilizer (Nitrophoska® Special 12–12–17, NPK-based)	WNPk
Plants irrigated with double-distilled water added with ammonium nitrate (YaraTera AMNITRA)	WAN
Plants irrigated with Plasma Activated Water	PAW
Plants inoculated with ToMMV and irrigated with double-distilled water	I-NTDDW
Plants inoculated with ToMMV and irrigated with Plasma Activated Water	I-PAW

$$\text{Chl } a \text{ (}\mu\text{g/mL)} = 11.24 A_{662} - 2.04 A_{645}$$

$$\text{Chl } b \text{ (}\mu\text{g/mL)} = 20.13 A_{645} - 4.19 A_{662}$$

$$\text{Chls (} a + b \text{) (}\mu\text{g/mL)} = 7.05 A_{662} + 18.09 A_{645}$$

$$\text{Car (}\mu\text{g/mL)} = (1000 A_{470} - 1.90 \text{Chl } a - 63.14 \text{Chl } b)/214$$

and the values were expressed as $\mu\text{g per g}$ of fresh weight of tissue.

For the ascorbate and glutathione pool content determination, plant samples were homogenized with three volumes of cold 5% (w/v) metaphosphoric acid in a porcelain mortar. The homogenate was centrifuged for 15 min at $20,000 \times g$ and the supernatant was collected for the analysis of ascorbate (AsA), dehydroascorbate (DHA), reduced glutathione (GSH) and oxidized glutathione (GSSG) according to Zhang and Kirkham [15].

2.6 Inoculation with ToMMV

Plants were artificially inoculated at 48 h after transplant and first irrigation. The inoculation was performed mechanically by abrasion with celite and a suspension of ToMMV obtained macerating by mortar and pestle 0.5 g of infected leaves at least 10 days post inoculation (dpi) in 2 mL of 0.1M Tris-HCl buffer pH 8.0. Plants were maintained until the expression of viral symptoms on inoculated plants (about 40 days after transplant).

2.7 RNA extraction and cDNA synthesis

Plant responses to PAW were studied by gene expression analysis carried out on uninoculated tomato plants at 24, 48, and 96 h from the first irrigation, and on uninoculated and ToMMV-inoculated plants at two and seven dpi. Three leaves were sampled from each of the three replicated pots for the untreated control and PAW-irrigated plants. Different seedlings were sampled at each time point to avoid the effects of the wounding stress. Total RNA was extracted from 50 mg of fresh tissues that were macerated in a 1.5 mL tube using a plastic pestle containing CTAB buffer added with 2% 40K-polyvinylpyrrolidone and 2% sodium metabisulfite just before use [16]. After chloroform extraction and isopropanol precipitation, the nucleic acid pellet was resuspended in sterile water and quantified by optical density reading with a NanoPhotometer™ N60 UV/Vis spectrophotometer (Implen, Germany).

Aliquots of 750 ng of the extracts were then reverse transcribed by MMLV-RT (Thermo Fisher Scientific, USA) and random hexanucleotide primers in a 40 μL reaction volume, at 42°C for 1 h, to obtain complementary DNA (cDNA).

2.8 Gene expression analysis

Plant defense-related genes were selected and used for gene expression analysis by quantitative polymerase chain reaction (qPCR). In detail, primer pairs specific for the four target genes (PAL [17], PR-1 [18], LOX [19], and CAT [20]), and for the reference genes elongation factor 1 α (EF-1) and ubiquitin (UBI) [21], were used. qPCR reaction mixture contained $1 \times \text{iQ}^{\text{TM}}$ SYBR® Green Supermix (Bio-Rad, Hercules, CA, United States), 25 μM of each forward and reverse primer, 1 μL of cDNA, and ultrapure water up to 25 μL .

PCR amplification was performed with the following cycling parameters: initial denaturation at 95°C for 3 min, 40 cycles at 95°C for 10 s, and 60°C for 45 s for annealing and extension. Melting curve analysis was performed over the range of 60°C–95°C. The stability of the two housekeeping genes was verified with BestKeeper® software [22] and the geometrical mean of both genes was used for gene expression analysis. The relative fold change was calculated according to the $2^{-\Delta\Delta\text{CT}}$ method [23].

2.9 Virus quantification

For qPCR quantification of ToMMV in tomato plants, the cDNA obtained as previously described and the primer set ToMMV-rtfor (5'-TTGTCATCAGCATGGGCCGACC-3', position 5759 > 5780 on the reference viral genome NC_022230) and ToMMV-rtrev (5'-ACACCTCGCTGAACTGCTGTTG-3', position 5854 > 5875) were used. The amplification mixture consisted of 1X SYBR™ Select Master mix (ThermoFisher Scientific, USA), 0.4 μM of each primer, 1 μL of cDNA, and ultrapure water up to 12.5 μL . A run of 40 cycles was performed with an annealing temperature of 56°C.

2.10 Micro- and macronutrients distribution in seedling leaves

The spatial distribution of several plant macronutrients (Mg, S, P, K, and Ca) and micronutrients (Mn, Fe, Cu, and Zn, data not shown) in tomato leaflets was investigated by collecting micro-focused X-ray

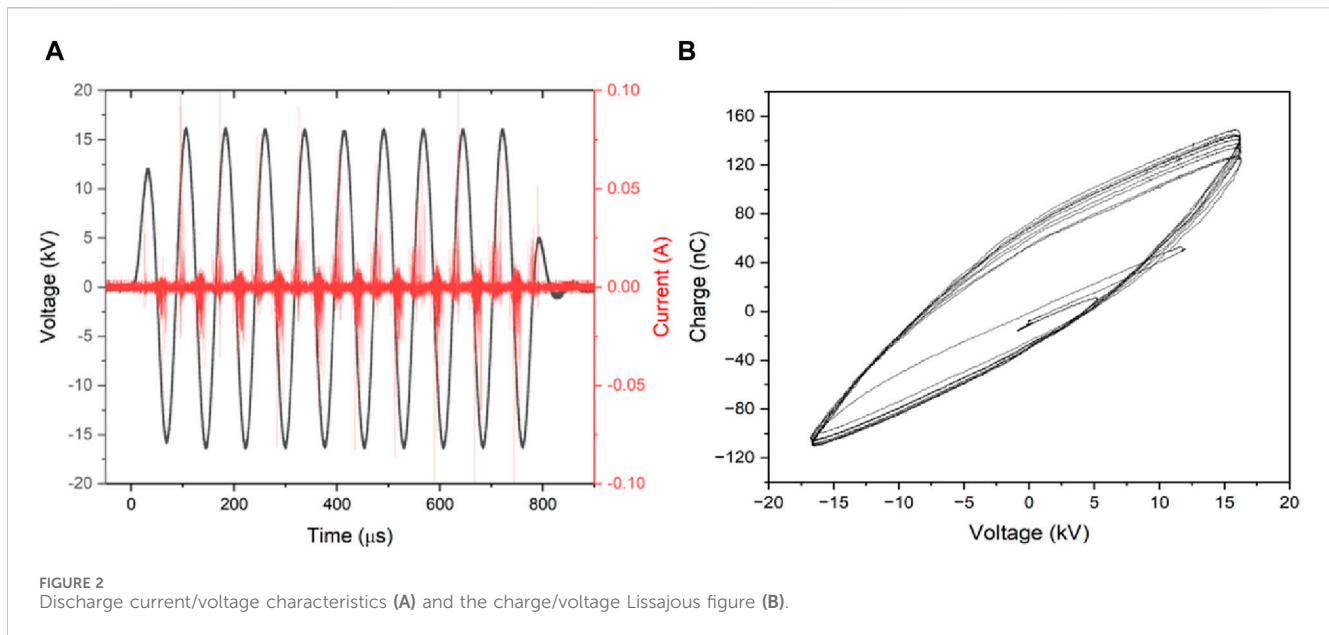


FIGURE 2 Discharge current/voltage characteristics (A) and the charge/voltage Lissajous figure (B).

fluorescence elemental maps. For such analysis, tomato leaves were collected from 40-day-old seedlings, the leaflets split and immediately prepared as described by Terzano et al. [24].

The μ -XRF analysis was carried out using a benchtop μ -XRF spectrometer (M4 Tornado, Bruker Nano GmbH, Berlin, Germany) equipped with a micro-focus Rh X-ray source (50 kV, 600 μ A), a polycapillary X-ray optics with a spot-size of 25 μ m and two Xflash™ energy dispersive silicon drift detectors (SDD) with 30 mm² sensitive area and an energy resolution of 140 eV @ Mn K α .

In particular, the following treatment conditions (as per Table 1) were analyzed: PAW, I-NTDDW, I-PAW, while WNPk and NTDDW were used as the positive and negative control, respectively. For each of the five sets of leaflets, rectangular areas of approximately 10 \times 15 mm at the middle right of the leaf and including the midrib were imaged by μ -XRF analyses.

All μ -XRF maps were acquired under near-vacuum conditions (20 mbar) using 25 μ m step size and 10 ms per pixel acquisition time. For each sample, the scanning was repeated 3 times, and the relative spectra were averaged to increase the signal-to-noise ratio (S/N). Finally, μ -XRF distribution maps were obtained with the ESPRIT software (Bruker Nano GmbH, Berlin, Germany, version 1.3.0.3273) and presented for each element using relative intensity scales.

2.11 Statistical analysis

The data reported are the average of three replicates from two independent biological experiments. For the investigated analyses, means and standard error (\pm ES) are shown. The Shapiro-Wilk test was run to verify the normality of data distribution. The analysis of variance (one-way ANOVA), followed by Tukey's *post hoc* test, was used to compare the conditions using GraphPad Prism version 9.0.0 for Windows (Boston, Massachusetts USA). Differences were considered statistically significant at a p -value ≤ 0.05 .

3 Results

3.1 Plasma characteristics

Panel A of Figure 2 displays the voltage and current waveforms observed during the PAW production treatment. The filamentary characteristics of the DBD are evident from the current peaks occurring at the onset of each voltage half-cycle. By integrating the obtained Lissajous figures (a typical one is presented in Figure 2B), we were able to estimate the energy dissipated during each voltage burst, resulting in a calculated value of $E_{\text{burst}} = 26$ mJ. Globally, over the course of the treatment, the water is subjected to a total plasma dose of 93.6 J/g_{water}.

3.2 Spectroscopic observation

In Figure 3 the emission spectra collected from the discharge zone above the water surface in air, in the spectral region from 270 to 420 nm, are reported.

They reveal strong bands of the second positive system (SPS) of molecular nitrogen and the first negative system (FNS) of molecular nitrogen ion, together with a clear signature of hydroxyl radical (OH) emission bands in the UV spectral region. In the Vis-NIR region, we observed characteristic sequences of bands of the first positive system (FPS) of molecular nitrogen together with the emission line for atomic oxygen observed at 777 nm (not shown). From the nitrogen SPS(0,0) band the rotational temperature was derived by using the spectroscopic tool Massive OES [25–27]. Figure 4 shows the experimental mean SPS(0,0) band profile, with corresponding standard error, together with synthetic profiles simulated for rotational temperatures of 444, 555, and 600 K respectively for the PIE observed in the corresponding gates. The estimated error from multiple simulations of bands, not shown for the sake of clarity, at different temperatures was on average of the order of 10% of the reported measurements being respectively ± 44 , ± 55 , and ± 60 . By comparing the acquired and simulated spectra, we can

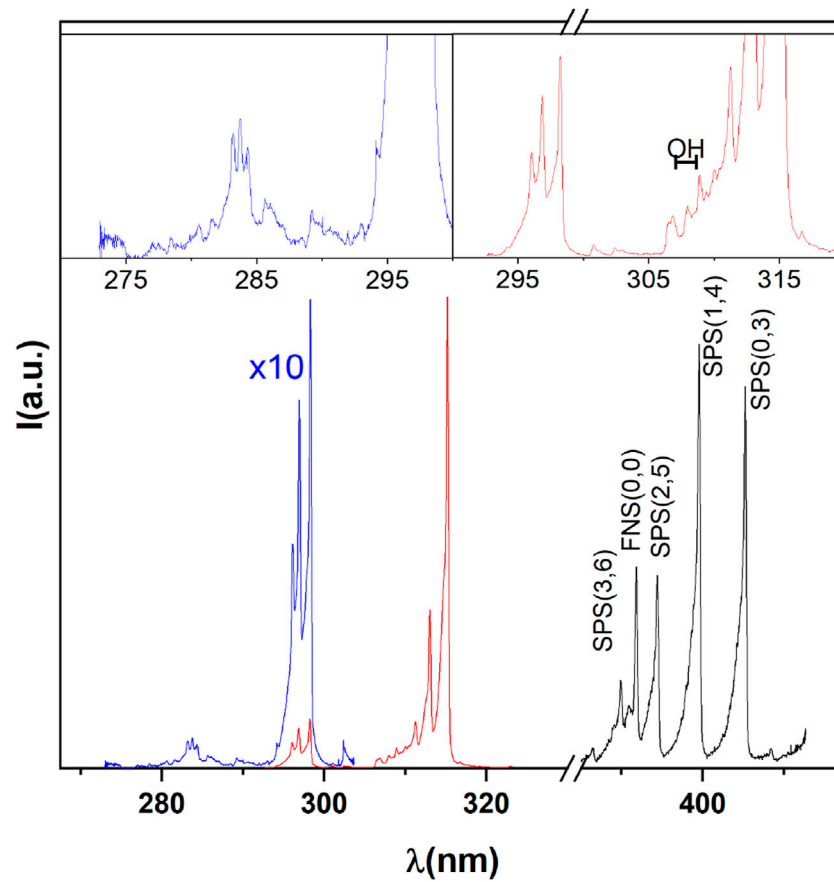


FIGURE 3 Spectral signature of the discharge.

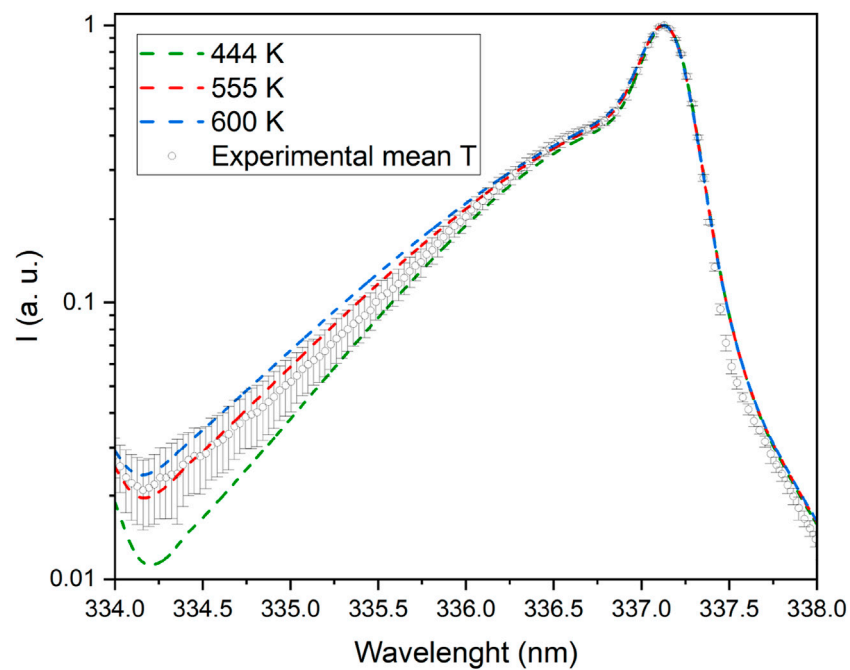


FIGURE 4 SPS(0,0) band signature for plasma temperature measurements.

surmise that the temperature developed in a plasma filament falls indeed in the 444–600 K range. However, it is also important to point out that, due to the filamentary character of the discharge, the temperature measured by optical emission is not representative of the entire volume of the gas inside the chamber but only of the portion of the gas crossed by the streamer. The treated water never reached the boiling point (save for possible local but not detected hot points), and its temperature increased by about 20°C (from 13,5 ± 0,8 to 35.3 ± 1.4°C) in all experiments.

3.3 PAW chemical composition

The chemical composition of PAW in terms of nitrite, nitrate, hydrogen peroxide concentration, pH, and ORP was characterized immediately after plasma treatments of 30 and 60 min. Subsequently, the measurements were repeated on water treated for 60 min 1 week after plasma treatment. This final measurement aimed to assess the chemical evolution of the PAW up to its equilibrium point. Figure 5 reports the analyses as mentioned above, grouped by measured quantity.

During the treatment, H₂O₂, NO₂⁻ and NO₃⁻ were produced, water was acidified and ORP increased. At higher treatment times [H₂O₂] increased and NO₂⁻ was converted into NO₃⁻ and other RNS.

pH and ORP in the PAW were quite stable after 1 week from the plasma treatment. [H₂O₂] and [NO₂⁻] decreased while [NO₃⁻] increased, likely due to a conversion of the first two compounds (i.e., NO₂⁻ oxidation) and other RNS into the latter.

The energy yield of NO_x production by our DBD setup is 2.7 g-NO_x kWh⁻¹. This translates into an energy efficiency of 81.2 MJ/mol NO_x just at the end of a 60-min plasma treatment, i.e. 1309.7 GJ/tN (tN = tons of nitrogen). This value, although somewhat high if compared to other studies focusing on plasma-catalytic nitrogen fixation, falls in ranges typical of NO_x production by DBD plasma without a catalyst [28,29].

3.4 Effects of irrigation with PAW on tomato plants

3.4.1 Biometric characteristics

Biometric parameters of tomato plants irrigated with PAW, in comparison with the other treatment conditions (WAN, WNPk, and NTDDW), were measured after 21 days of treatment. Figure 6 reports a representative example of samples grown in different conditions. Results, reported in Figure 7, show that the PAW treatment performs better in terms of stem length, diameter, and leaf area surface with statistically significant differences with respect to the other cases. No significant differences are obtained among the other cases.

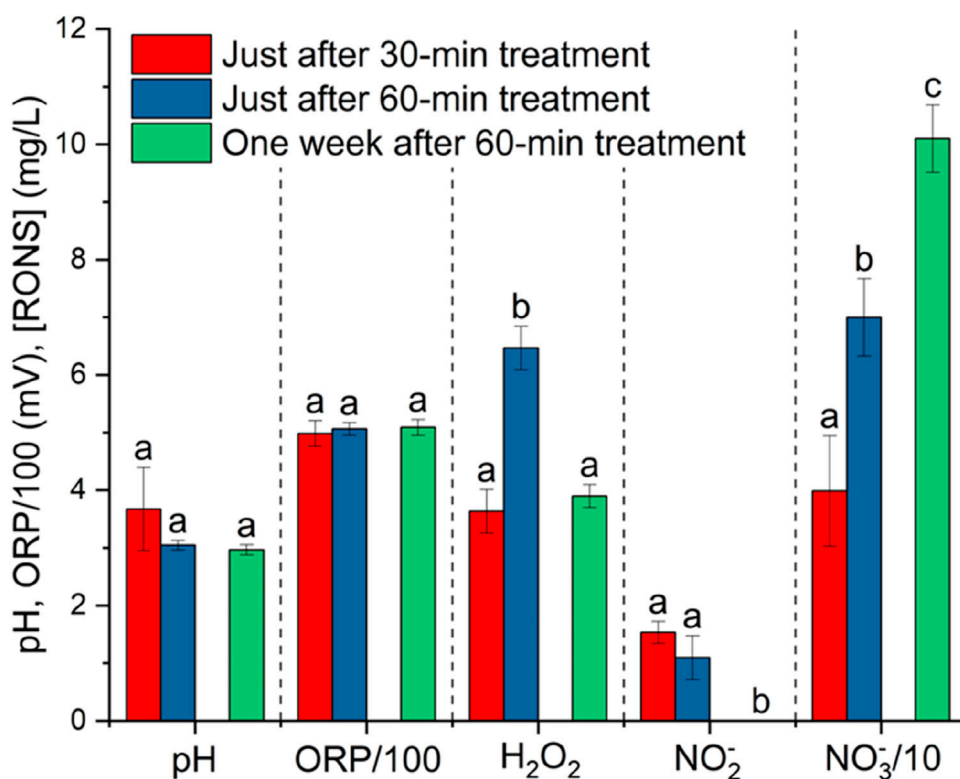


FIGURE 5 pH, ORP, nitrate, nitrite, and hydrogen peroxide content of PAW at two different water-treatment times (30 and 60 min) and 1 week after a 60-min plasma treatment. The 500 mL samples used for this measurements were stored in the dark at room temperature following treatment. Values with the same letter for each parameter are not significantly different by Tukey's HSD test ($p < 0.05$).

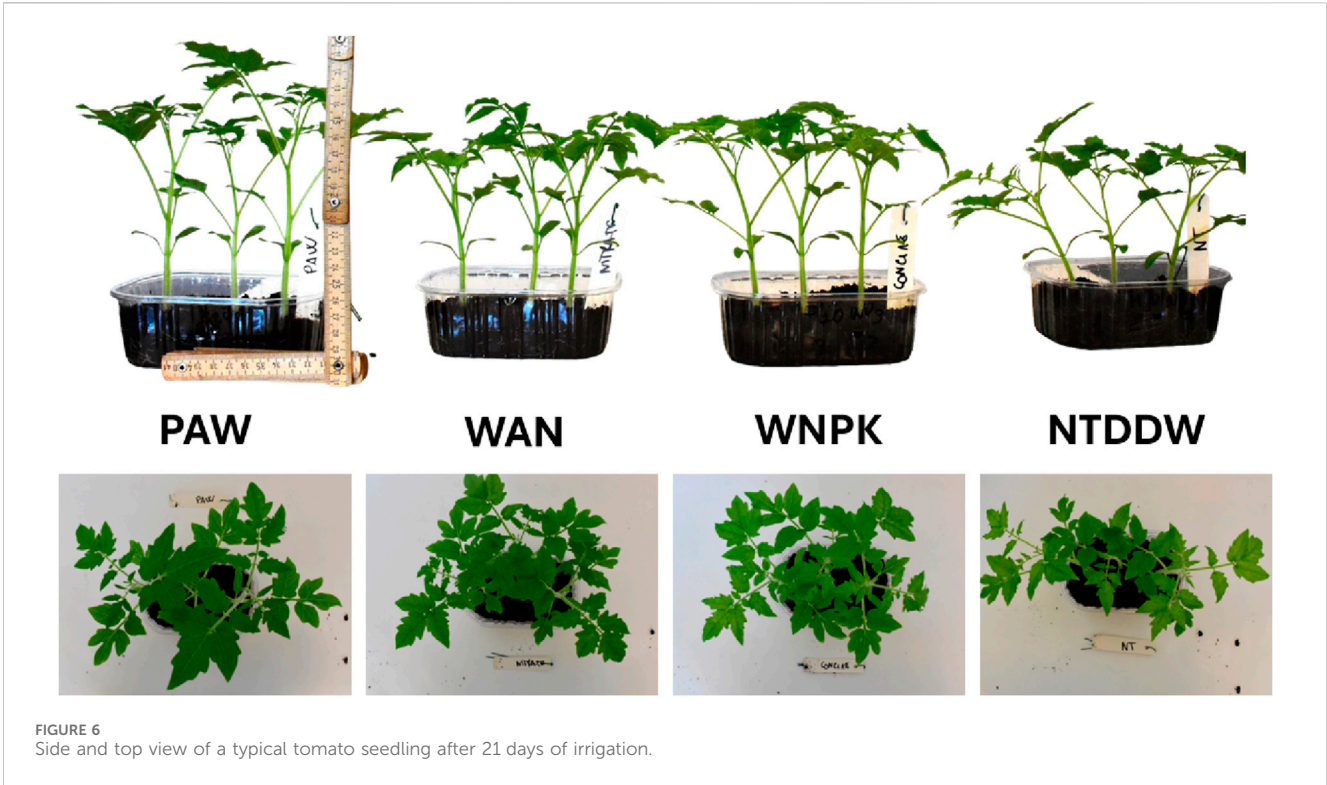


FIGURE 6 Side and top view of a typical tomato seedling after 21 days of irrigation.

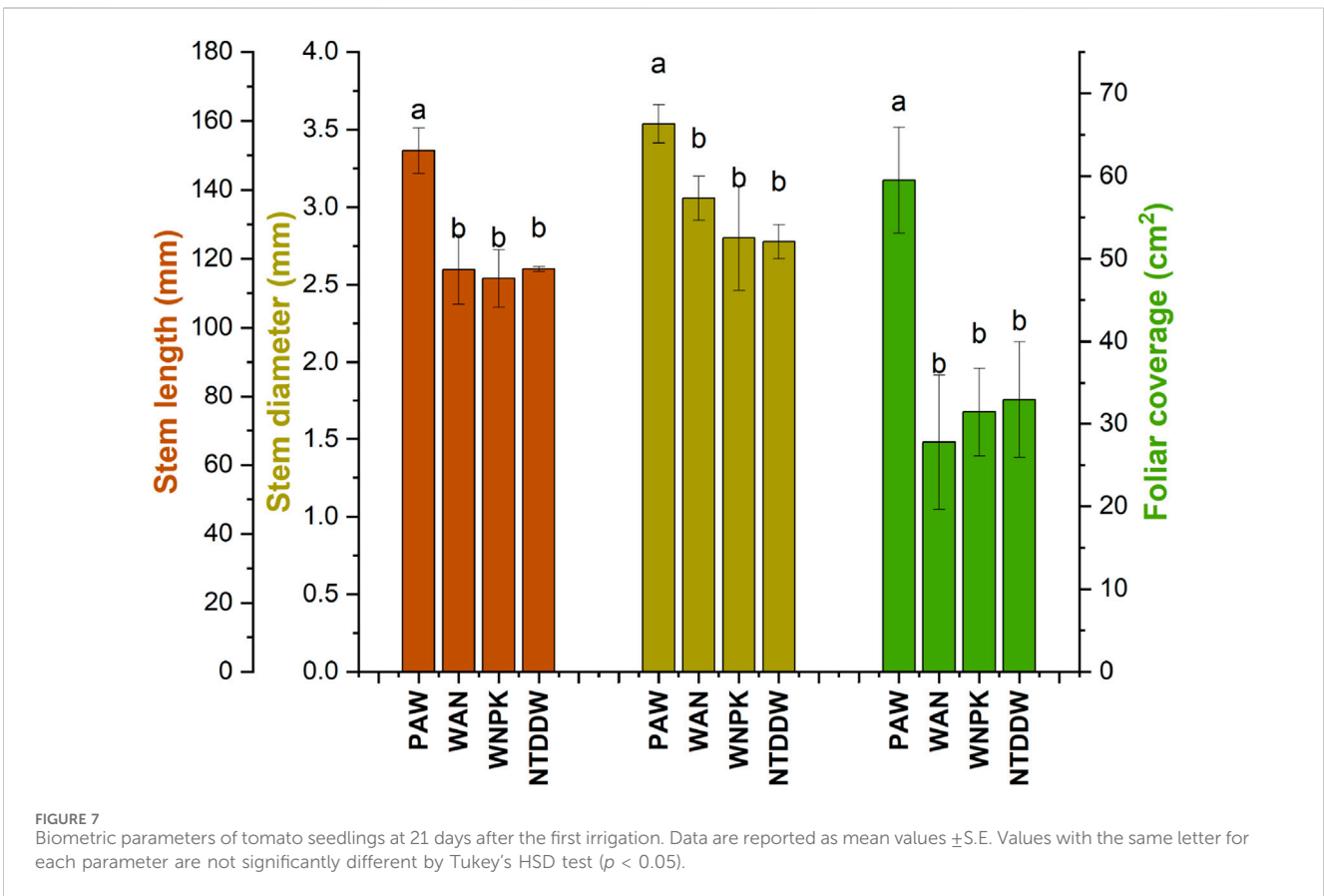


FIGURE 7 Biometric parameters of tomato seedlings at 21 days after the first irrigation. Data are reported as mean values \pm S.E. Values with the same letter for each parameter are not significantly different by Tukey's HSD test ($p < 0.05$).

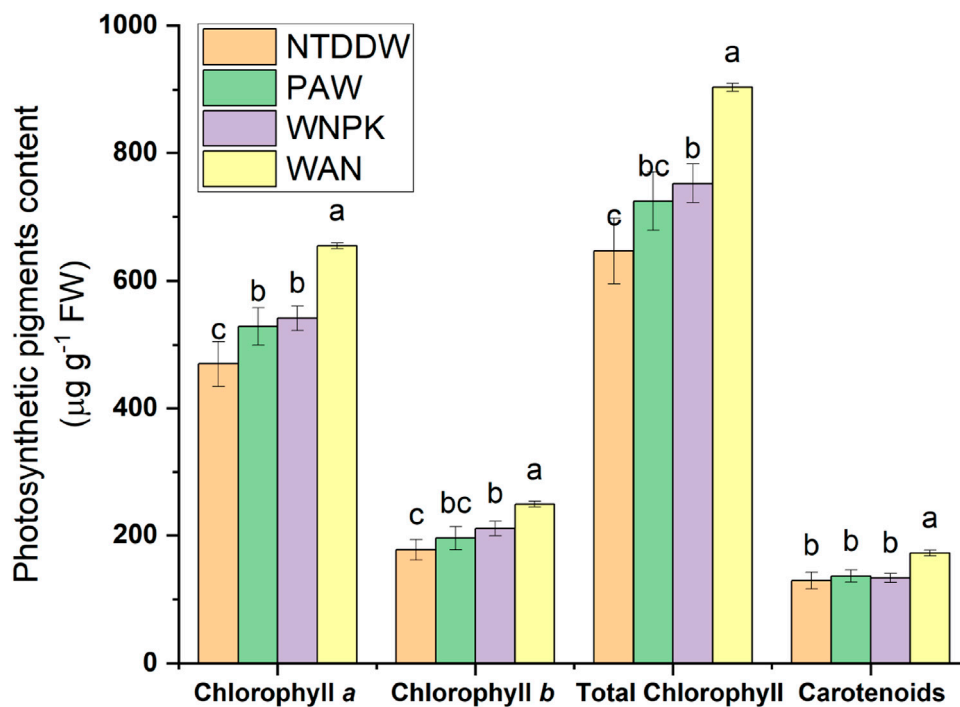


FIGURE 8
Photosynthetic pigments content at 21 days after the first irrigation. Data are reported as mean values \pm S.E. Values with the same letter are not significantly different by Tukey's HSD test ($p < 0.05$).

3.4.2 Effect of different treatments on photosynthetic pigments

In all treatments, a significant increase of chl *a* respect to the control NTDDW was observed (see Figure 8). Chl *b* and total chlorophyll (*a* + *b*) increased in WNPk and more significantly in WAN while no significant changes were observed for the PAW samples with respect to the NTDDW. Carotenoids significantly increased in WAN samples whereas in PAW and WNPk samples, no difference with respect to the control was recorded.

3.4.3 Changes in ascorbate and glutathione pool

The changes in reduced (AsA) and oxidized (DHA) ascorbate forms together with the total pool after treatments are shown in Figure 9A. Tomato seedlings exposed to PAW showed the highest pool content (AsA + DHA) compared to the NTDDW control and other treatments. Particularly, both the reduced and oxidized forms of ascorbic acid were highest ($p < 0.05$) in seedlings treated with PAW. The same levels of AsA total pool and AsA were observed in the WAN sample if compared to the control NTDDW. As regards the WNPk sample, AsA content significantly decreased with respect to NTDDW whereas DHA content did not change with a consequent decrease of AsA total pool. A significant decrease in the AsA/(AsA + DHA) ratio occurred in WAN while no change in the other treatments with respect to the control NTDDW was registered (Figure 9B).

In the seedlings treated with WNPk and WAN, both the reduced (GSH) and oxidized (GSSG) glutathione forms significantly decreased with respect to the control NTDDW, and consequently, a decrease in

glutathione pool was observed (Figure 9C). In the PAW treatment, no difference in GSH and GSSG content was observed, if compared to the control NTDDW. In addition, a decrease in the GSH/(GSH + GSSG) ratio was registered in WNPk and WAN treatments if compared to PAW and NTDDW ones (Figure 9D).

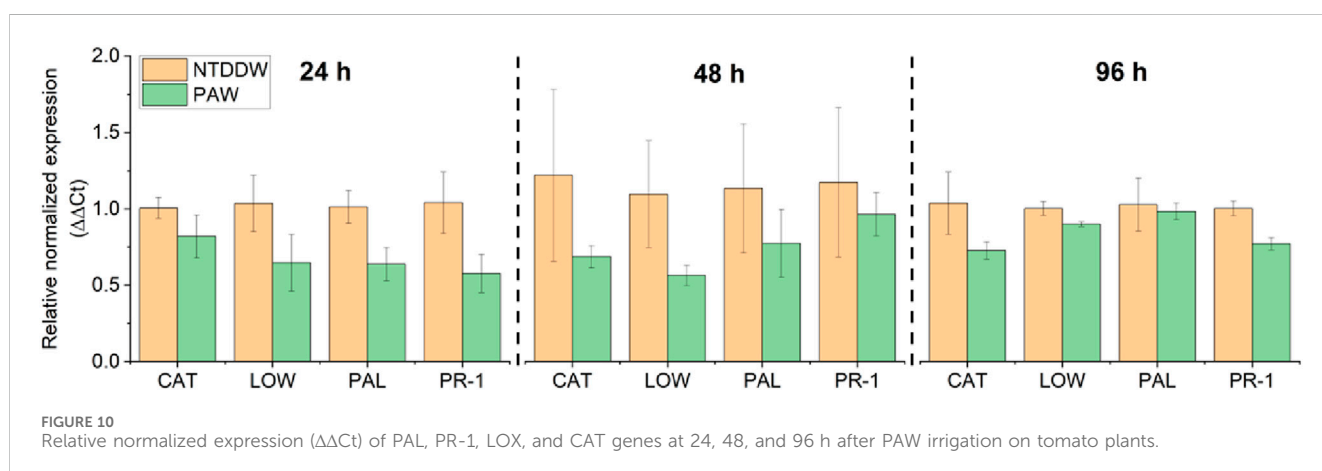
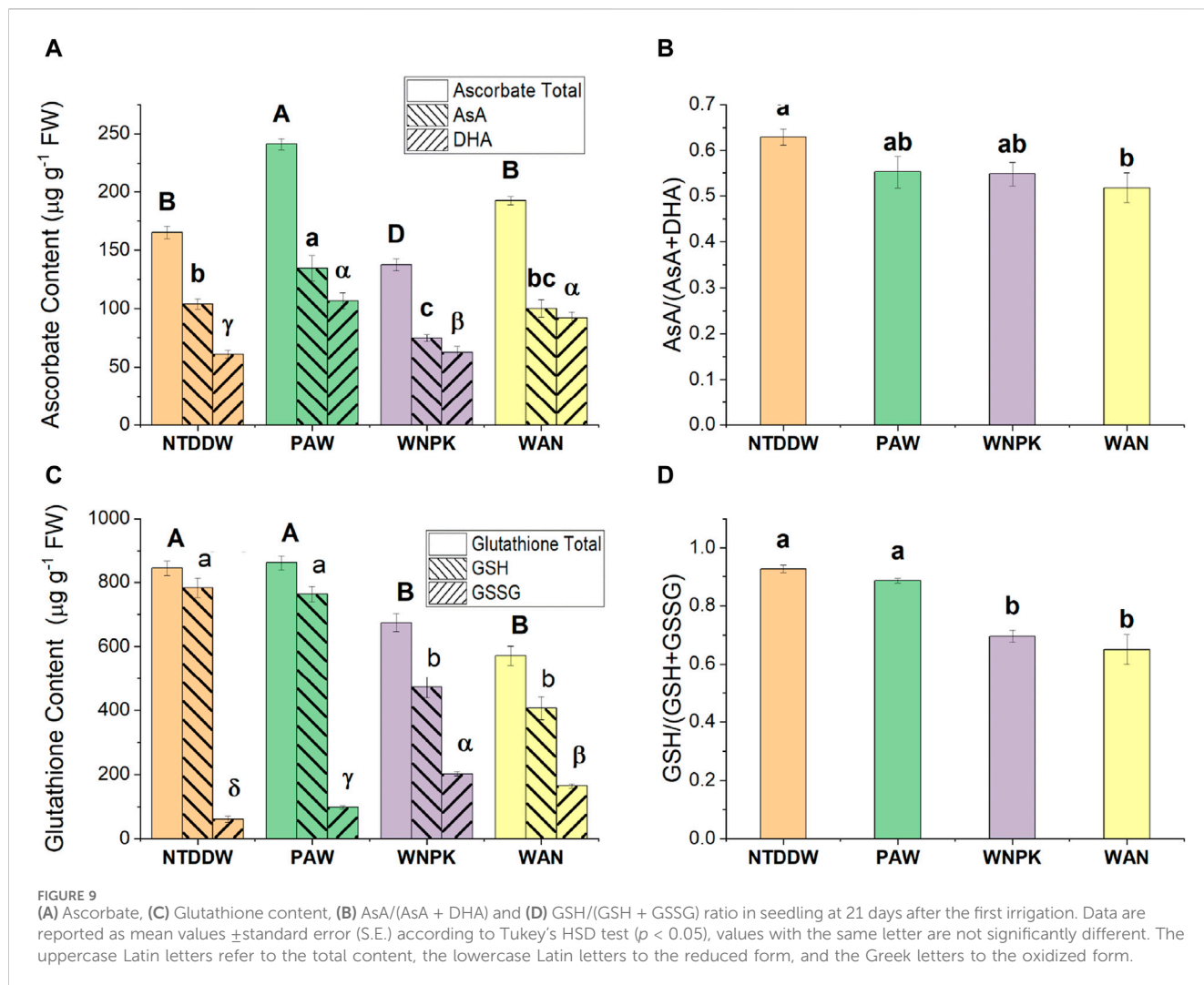
3.4.4 Gene expression analysis in tomato plants irrigated with PAW

To evaluate the possible induction of defense-related genes after irrigation with PAW, the relative normalized expression ($\Delta\Delta C_t$, related to the untreated control) of the PAL, PR-1, LOX, and CAT genes was analyzed.

In un-inoculated plants analyzed at early stages (24, 48, and 96 h) after watering, all four genes were downregulated in the PAW-irrigated plants compared to the control (NTDDW) (Figure 10). Fewer differences in gene expression between the two conditions were generally recorded at 96 h compared to the previous sampling times (Figure 10).

On the contrary, in the ToMMV-inoculated plants analyzed at two and seven dpi, all the genes were upregulated by irrigation with PAW (Figure 11, right panel). In particular, the highest upregulation induced by PAW was recorded for PR-1 and LOX genes at seven dpi, with a mean fold change (FC) of gene expression levels close to two for both genes.

At two dpi, on the uninoculated plants (Figure 11, left panel) the PR-1 gene was upregulated (FC = 1.4), while the other genes were only slightly upregulated (CAT and LOX) or downregulated (PAL) by PAW. At seven dpi, all the genes were slightly downregulated in PAW compared to NTDDW samples.



3.4.5 Virus quantification

Virus concentration in the inoculated plants increased along with the sampling time points because of the viral replication in the infected tissues. Thus, the quantification cycle (C_q) at which the titer started to be visible over the threshold of negative values, decreased

from two dpi to seven dpi in both I-PAW (PAW-treated virus-inoculated) and I-NTDDW (untreated-inoculated) samples. A trend of a slight increase in virus concentration was apparently visible, however, in I-PAW, showing C_q values ranging from 19.97 (2 dpi) to 10.25 (7 dpi), compared to I-NTDDW, with C_q values from

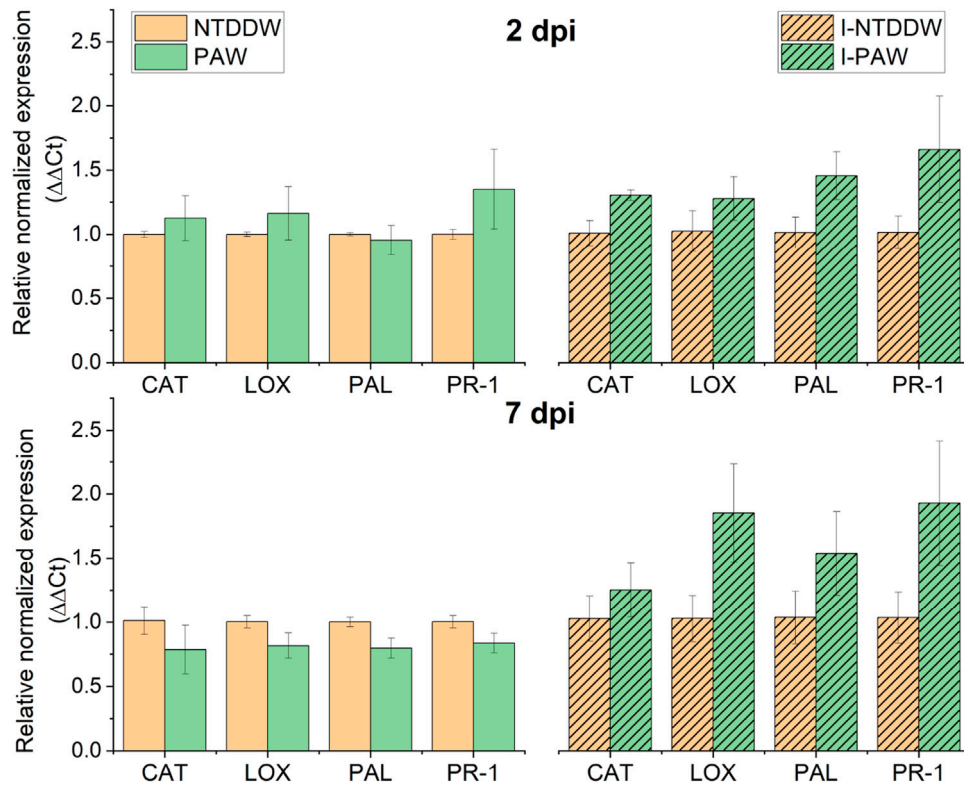


FIGURE 11 Relative normalized expression ($\Delta\Delta Ct$) of PAL, PR-1, LOX, and CAT genes in uninoculated, untreated (NTDDW) and treated (PAW) plants, and in inoculated, untreated (I-NTDDW) and treated (I-PAW) plants, at two and seven dpi (days after inoculation) with Tomato mottle mosaic virus (ToMMV).

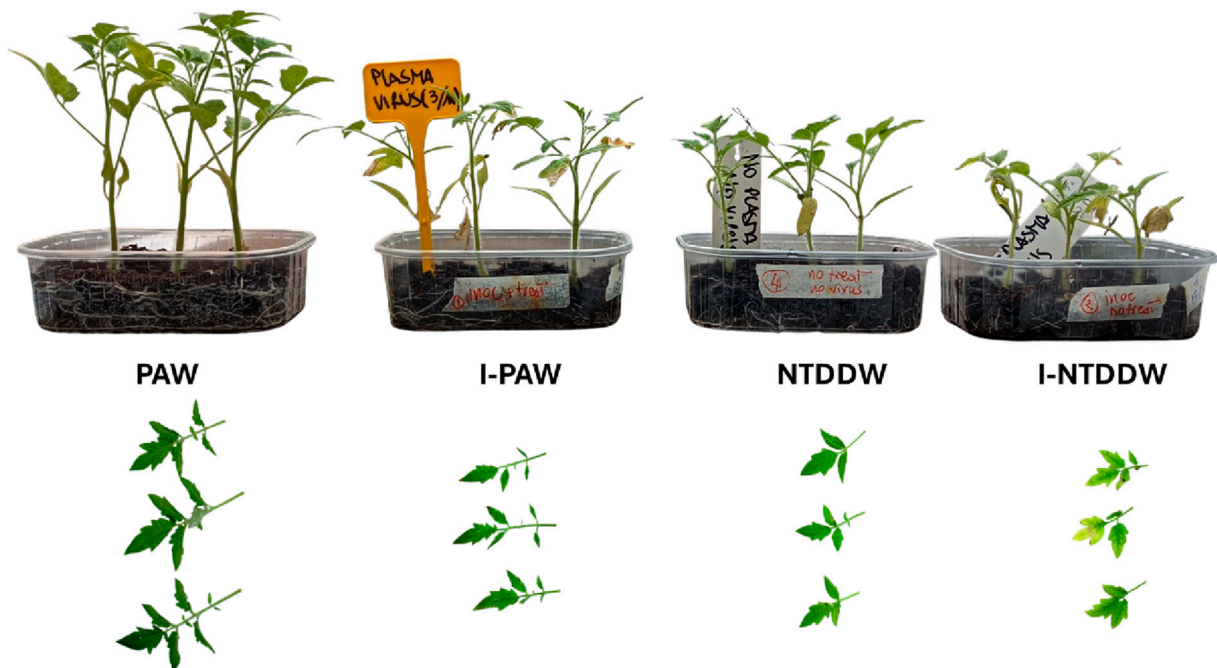


FIGURE 12 On the top row, the typical plant growth of the four reported cases at the time of the show-up of the disease symptoms. On the bottom row, pictures of the sampled leaves for μ -XRF analysis.

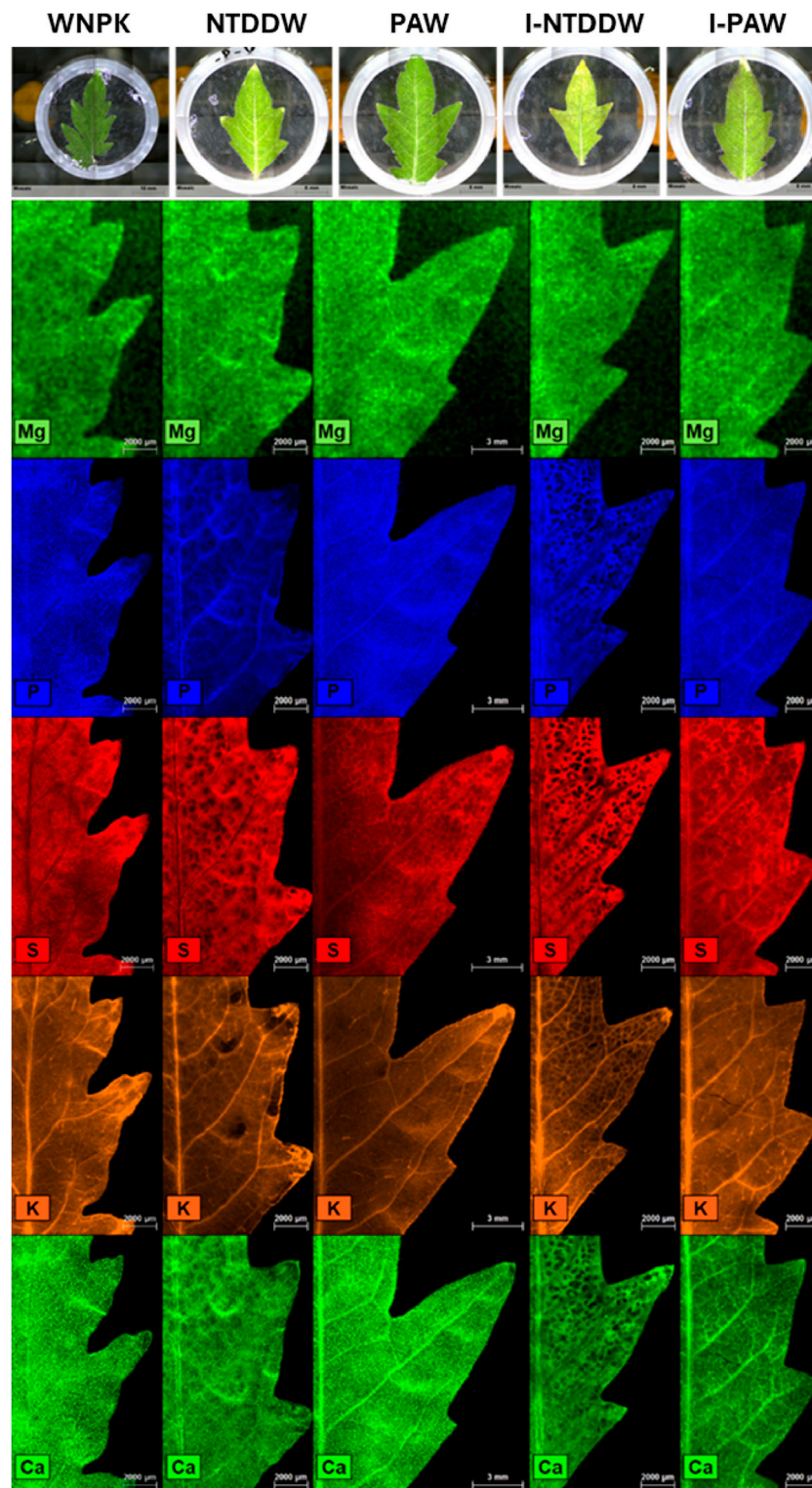


FIGURE 13
Spatial distribution of Mg, P, S, K, and Ca in tomato leaflets, as obtained through μ -XRF analysis.

19.07 to 11.87 at the same time points. No virus infection was detected in uninoculated plants (PAW and NTDDW). The expression of symptoms on inoculated plants (stunting, shoe-stringed and mottled

leaves, generalized yellowing of the foliage, etc.) started to be visible after 35–40 dpi because the cultivar Regina (a local variety) used in the trials could be considered quite tolerant to the ToMMV infection [30].

3.4.6 Micro and macronutrients distribution in seedling leaves

In this study, μ -XRF was applied to investigate the possible effects of PAW on element homeostasis at the leaf level, also in the case of ToMMV infection. Figure 12 captures the status of the seedlings at 40 days after transplanting for the PAW, I-PAW, NTDDW, and I-NTDDW cases. Figure 13 shows the spatial distribution of Mg, P, S, K, and Ca in tomato leaflets, as obtained through μ -XRF analysis. For the above-listed elements, the positive control sample (WNPK) shows a rather homogeneous distribution in the different leaf tissues, which in general can be considered indicative of good nutritional and health status [31]. Similar distributions can be observed in PAW samples too, even if some differences occur in the I-PAW leaflet, especially for Ca. Indeed, Ca distribution in I-PAW seems to be partially affected by the ToMMV, with a preferential accumulation of this element in the veins rather than in the leaf lamina. Along with this, in both PAW and I-PAW samples also the S signal increased in the midrib and primary veins with respect to the WNPK. Conversely, in the WNPK and untreated (NTDDW and I-NTDDW) samples, S is not observed in the veins. Besides this, other significant differences were clearly visible in untreated samples (NTDDW and I-NTDDW) when compared to the positive control (WNPK) and the treated ones (PAW, I-PAW). In fact, for all the untreated samples, inhomogeneous element distributions at the leaf level were observed especially for P, S, and Ca, characterized by large dark spots in the distribution maps. Potassium (K) distribution also shows several depletion zones in untreated samples, with fewer but larger dark spots for NTDDW, becoming smaller but more frequent in I-NTDDW. These phenomena appeared more intense for the inoculated samples (Figure 13).

4 Discussion

In this paper, we evaluated Plasma Activated Water (PAW) as a novel irrigation medium to promote growth and defense responses in tomato seedlings, either healthy or inoculated with ToMMV. Plasma-based technologies could pose an interesting and viable alternative to traditional fertilizing methods, by their nature as on/off sources that do not require the employment of chemicals and eliminate the need for stockage [32].

PAW was produced by exposing double-distilled water to a VDBD plasma in a custom-made reactor. The “activation” process involves chemical species that are produced at the onset of the plasma discharge. The main reactants in the gas phase that are exposed to plasma are molecular oxygen and nitrogen, from the supplied air, and water vapor. When the discharge is ignited, these molecules are immediately vibrationally excited, and the energy provided by the plasma breaks them apart and fosters a series of reaction pathways that are not yet fully understood. For example, from the spectroscopic observations we reported, we can infer the formation of NO, atomic oxygen, and hydroxyl radicals near the discharge filaments. These species are then dissolved in the water bulk through the water-gas interface, where they continue to undergo a series of reactions and chemical transformations. As reported by Lukes et al. [33], the transient species produced in the discharge (namely, OH, NO, and NO₂ radicals) are converted into

more stable chemical products once they are dissolved in water, such as H₂O₂, NO₂⁻ and NO₃⁻, acidifying the produced PAW. At the acidic pH values that are typical of the produced PAW, moreover, a conversion mechanism of H₂O₂ and NO₂⁻ into NO₃⁻ through the peroxyxynitrite intermediate is established [33], leading to the depletion of hydrogen peroxide and nitrite ion and an increase in the concentration of nitrate ion at longer treatment times. A week after the PAW production, this reaction results in the complete disappearance of NO₂⁻, a decrease of the H₂O₂ content in the PAW, and conversely, an increase in NO₃⁻. The acidity (pH 3.0 ± 0.1) after complete treatment of the solution can be attributed mainly to nitric acid. However, the acidic nature of PAW is not a problem when used to water plants grown on soil or a solid substrate since soils and substrates usually have a buffer capacity that prevents substrate acidification or strongly limits pH variations, such as in the case of our study. A proper selection of soil and substrate, as it is usually done in horticulture, is therefore important to get a final pH that is suitable for the growth of the selected crop. In addition, NO₃⁻ uptake by plant roots occurs through a symport transport with H⁺ ions which causes an increase of pH of the growth medium [34]. Being nitrogen mainly in the form of NO₃⁻ in PAW, such physiological process contributes to balance PAW acidity. Differently, more attention should be paid when PAW is used in hydroponic systems. In this case, the solution should be properly buffered (e.g., by adding other mineral nutrients as base salts or metals with catalytic properties for nitrogen fixation [35,36]) before use.

The measured ORP of 506 ± 11 mV, which suggests an oxidizing character of the PAW, is caused by the presence of all the above-mentioned species, known to possess highly oxidative properties. The typical ORP value of the PAW could prove useful in the decontamination of soils against plant pathogens to prevent and manage soilborne diseases and could also put the plant cell into mild oxidative stress, unlocking new metabolic pathways for growth and defense responses conferring resistance to biotic and abiotic stresses.

Biometric measurements were performed on plants after 21 days of irrigation for the four different treatment conditions. Results showed a statistically different behavior of PAW irrigated samples with respect to other conventional treatments and untreated ones. In particular, the growth of PAW-irrigated seedlings was enhanced by at least 10% for all the measured parameters. Moreover, to evaluate the effect of PAW on the fitness of the seedlings after 21 days of treatment, antioxidant molecules such as ascorbic acid and glutathione and pigments such as chlorophylls and carotenoids were also monitored.

Chlorophylls and carotenoids are pigments that with proteins form the light-harvesting complexes that are part of photosystems, functional units of photosynthesis [37]. Although WNPK and WAN induced an increase in both chl *a* and *b* implying a higher photosynthetic activity, the higher increase of chl *a* than chl *b* in the PAW treatment suggests in the latter an easier translocation of energy from chl *b* to chl *a*. This trend facilitates the irreversible direction in the energy capture process making the energy transfer of light excitation to the reaction center more efficient.

As a consequence, this could lead to higher production of NADPH and ATP in the light-dependent reactions (first stage of the photosynthesis) and their increased availability for the Calvin cycle (second stage of the photosynthesis) with higher production of photosynthates (such as sucrose), necessary for plant growth and

productivity. The sugar sucrose is a source of glucose which is the substrate, in the Smirnoff-Wheeler pathway, for vitamin C biosynthesis in plants [38] that, in our study, increased in PAW-treated seedlings. The presence of ascorbate is associated with preserving the photosynthetic process [39] and limiting ROS-mediated damage and leaf senescence [40]. The decrease in chlorophyll a was linked to reductions in AsA content, leading to decreased RuBisCO activity and CO₂ assimilation [40].

It is known that an augmented carotenoid level could be correlated to counteract the damage to the photosynthetic apparatus induced by UV light [41]. The fact that an increase of carotenoid content in PAW was not observed as compared to WAN, could therefore suggest the absence of relevant perturbations in the light-harvesting complex and the energy transfer towards the reaction center [37].

Ascorbate and glutathione are part of the ascorbate-glutathione cycle [42] and are the most abundant low molecular-weight antioxidants in plant cells. They regulate the concentration of the reactive oxygen species in plant cells, particularly hydrogen peroxide [38]; however, they are multifaceted molecules involved in various processes such as plant growth and defense [43]. The higher content of AsA in tomato seedlings irrigated with PAW strongly suggests the role of PAW in promoting the production of this antioxidant compound. On the other hand, the content of reduced glutathione (GSH - another important antioxidant metabolite of the plant) and glutathione pool (GSH + GSSG) remained unchanged in the presence of PAW with respect to the NTDDW control, suggesting a more relevant involvement of AsA rather than GSH in the PAW-modified plant metabolism, confirming the prominent role of ascorbate in the plant defense responses [44,45]. AsA, counteracting the oxidative stress in cells, underlines its key role played in the tolerance to several biotic and abiotic stresses [46]. The decreased GSH content in both WNPK and WAN samples with the contemporaneous higher GSSG production contributed to a shift in the redox state of this metabolite towards the oxidative form with consequent higher oxidized cell status [47] in those seedlings.

The possible induction of genes implicated in plant defense by irrigation of tomato seedlings with PAW was investigated at different time points. Transcript changes of the analyzed genes, including PR-1 and PAL with a key role in defense responses to pathogens, LOX, and the antioxidant enzyme CAT, were compared between treated and untreated control plants. In particular, PR-1 is a molecular marker for the salicylic acid-activated pathway that is rapidly and strongly induced as a response to pathogen infections [48]. All four genes were not activated, in our experiments, during the early stages after plant exposure to PAW. However, the plants irrigated with PAW showed a significant upregulation of the majority of the genes, slightly predominant for PR-1, following inoculation with the virus ToMMV, suggesting an effect of priming of induced defense responses by the treatment [49]. This could suggest that the activation of plant defense responses, possibly primed by reactive species in PAW, should allow the treated plants to be more promptly reactive against pathogens. In the uninoculated condition, downregulation of the same genes in treated vs. untreated samples could be likely due to the activation in treated plants of primary metabolism responsible for plant growth and development instead of that related to defenses [31].

In the cultivar Regina we used for the test, which is a traditional, long-lasting local variety in our region, the symptoms expression appeared very late in the time frame chosen for our experimental plan and, thus, it could be considered tolerant to ToMMV infection. Significant symptoms we observed, such as green mottling, shoe-string leaves, and stunting, started to be visible at least 3 weeks after inoculation. The comparison between I-PAW and I-NTDDW showed indeed a higher virus accumulation rate, with an increase in the former rather than in the latter. It can be hypothesized that the infection of a tobamovirus, having such an active replication and accumulation in the infected tissues, is somehow favored by an overall better nutritional status and nutrient mobilization as promoted by the PAW treatment. It could mean that the plants watered with PAW uptake higher amounts of nutrients (e.g., mineral elements) to support and even enhance the virus replication in well-nourished tissues.

In plants, disorders in element homeostasis at the leaf level are often correlated to nutritional deficiencies, the presence of pathogens (including viruses), environmental stresses, etc. Observing the changes in the spatial distribution of certain macro and/or micronutrients can provide valuable information for understanding the type and the impact of the stressor. For such investigations, μ -XRF is an essential and effective technique [31]. Significant changes in elemental distribution were observed in μ -XRF maps for P, S, Ca, and K in the virus-inoculated sample watered only with distilled water (I-NTDDW) as compared to a nutrient-sufficient uninoculated plant (WNPK), showing several spotted depletion zones. The lack (or lower concentration) of these important macronutrients in many leaf cells provides evidence of the virus infection, resulting in the already mentioned visual symptoms such as stunting, shoe-stringed and mottled leaves, and generalized yellowing of the foliage. Yet, some inhomogeneities in element distribution could be also observed in the plants watered only with double-distilled water (NTDDW), suggesting nutrient deficiencies, as compared to the nutrient-sufficient control (WNPK). However, the virus inoculation appeared to worsen the pre-existing nutritional stress status, with an evident increase in the size and number of nutrients-depleted areas (Figure 13). Such inhomogeneous distributions are not evident in the PAW watered samples, thus suggesting that PAW can provide a sufficient level of nutrients to tomato plants, similar to what happens to the plants irrigated with a solution containing the chemical fertilizer (WNPK). In addition, the irrigation of virus-inoculated plants with PAW (I-PAW) appeared to almost completely restore the mineral nutrients distribution in tomato leaves, becoming more similar to that of the control healthy plant (WNPK).

Finally, the S distribution in PAW-treated plants, either inoculated or uninoculated, showed that S concentration increased in leaf veins, suggesting a mobilization of S-containing compounds (e.g., glutathione) from plant leaves through the phloem. Indeed, S assimilated in leaves is exported via the phloem to sites of protein synthesis (shoot and root apices, and fruits) mainly as glutathione [34] which can also act as a non-enzymatic antioxidant that can be activated to overcome oxidative perturbations [50] like those induced by PAW.

The results of this study regarding the PAW's effects on plant growth and defense responses are in accordance with previous

studies [9–12]. Generally, the results indicate the presence of a better physiological status of the PAW-treated plants to cope with oxidative stress and maintain cellular homeostasis. The augmented chlorophyll *a* content with the increase of antioxidant molecules such as the ascorbate suggests that PAW treatment can potentiate the plant defense and contribute to higher sugar production, necessary for plant growth and productivity. In agreement with our results, an enhancement of plant defense responses induced by PAW treatment has been also reported by several authors [12,51]. Overall, these findings highlight the potential of PAW as a sustainable and innovative irrigation medium for enhancing plant performance and resilience in the face of environmental challenges. However, additional studies regarding the involvement and effect of PAW on other antioxidant systems (such as enzymatic activity, and phenols) and metabolic pathways (such as sugar synthesis) are necessary to better understand the potential of PAW in the plant systems.

5 Conclusion

This thorough exploration, encompassing both healthy and virus-stressed conditions, provides a more detailed understanding of the dynamic interplay between PAW and tomato plant growth. Our findings aim to contribute not only to the growing body of knowledge surrounding the applications of PAW but also to the specific insights into its potential as a stress-alleviating agent in the context of viral infections. Through the examination of plant development, biochemical responses, nutrient dynamics, and gene expression patterns, our research provides further evidence of the role of PAW as a sustainable alternative to conventional chemicals used in agriculture. Furthermore, the over-expression of the defense-related genes of plants irrigated with PAW suggests that the crop resilience to pathogenic challenges could be enhanced potentially reducing crop losses on the field.

Data availability statement

The original contributions presented in the study are included in the article/Supplementary material, further inquiries can be directed to the corresponding author.

Author contributions

DA: Data curation, Investigation, Writing–review and editing, Formal Analysis, Methodology, Validation. PR: Data curation, Formal Analysis, Investigation, Validation, Writing–review and editing, Methodology. CP: Data curation, Investigation, Methodology, Writing–review and editing, Formal Analysis. BB:

Data curation, Investigation, Methodology, Writing–review and editing. CP: Formal Analysis, Methodology, Validation, Writing–review and editing, Resources, Data curation. RT: Data curation, Formal Analysis, Methodology, Validation, Writing–review and editing, Funding acquisition, Resources. AM: Conceptualization, Formal Analysis, Methodology, Writing–review and editing, Funding acquisition, Data curation, Investigation. MA: Data curation, Investigation, Writing–review and editing. GD: Formal Analysis, Methodology, Validation, Writing–review and editing. BL: Investigation, Methodology, Writing–review and editing. RD: Writing–review and editing, Data curation, Formal Analysis, Funding acquisition, Methodology, Resources, Validation, Conceptualization. PA: Conceptualization, Data curation, Funding acquisition, Investigation, Supervision, Writing–original draft, Writing–review and editing, Resources, Validation.

Funding

The author(s) declare that financial support was received for the research, authorship, and/or publication of this article. Open access funding provided by MUR-Fondo Promozione e Sviluppo – DM 737/2021 CUP H99J21017820005 funded by European Union – Next Generation EU PlaTEC. We acknowledge: European Cooperation in Science and Technology, CA19110; Regione Puglia, Riparti - POC PUGLIA FESRT-FSE 2014/2020; Ministero dello Sviluppo Economico, F/050421/01–03/X32 Protection; Ministero dell’Istruzione, dell’Università e della Ricerca, PONa3_00369 SISTEMA; Agritech National Research Center funding from the European Union Next-Generation EU (PIANO NAZIONALE DI RIPRESA E RESILIENZA (PNRR) –MISSIONE 4 COMPONENTE 2, INVESTIMENTO 1.4–D.D. 1032 17/06/2022, CUP H93C22000440007, CN00000022).

Conflict of interest

The authors declare that the research was conducted in the absence of any commercial or financial relationships that could be construed as a potential conflict of interest.

The author(s) declared that they were an editorial board member of *Frontiers*, at the time of submission. This had no impact on the peer review process and the final decision.

Publisher’s note

All claims expressed in this article are solely those of the authors and do not necessarily represent those of their affiliated organizations, or those of the publisher, the editors and the reviewers. Any product that may be evaluated in this article, or claim that may be made by its manufacturer, is not guaranteed or endorsed by the publisher.

References

- Konchev EM, Gusein-zade N, Burmistrov DE, Kolik LV, Dorokhov AS, Izmailov AY, et al. Advancements in plasma agriculture: a review of recent studies. *Int J Mol Sci* (2023) 24:15093. doi:10.3390/ijms242015093
- Ambrico PF, Šimek M, Ambrico M, Morano M, Prukner V, Minafra A, et al. On the air atmospheric pressure plasma treatment effect on the physiology, germination and seedlings of basil seeds. *J Phys D Appl Phys* (2020) 53:104001. doi:10.1088/1361-6463/ab5b1b
- Ambrico PF, Šimek M, Morano M, De Miccolis Angelini RM, Minafra A, Trotti P, et al. Reduction of microbial contamination and improvement of germination of sweet basil (*Ocimum basilicum* L.) seeds via surface dielectric barrier discharge. *J Phys D Appl Phys* (2017) 50:305401. doi:10.1088/1361-6463/aa77c8
- Misra NN, Schlüter O, Cullen PJ. Plasma in food and agriculture. In: *Cold plasma in food and agriculture*. Elsevier (2016). p. 1–16. doi:10.1016/B978-0-12-801365-6.00001-9
- Zhou R, Zhou R, Prasad K, Fang Z, Speight R, Bazaka K, et al. Cold atmospheric plasma activated water as a prospective disinfectant: the crucial role of peroxydinitrite. *Green Chem* (2018) 20:5276–84. doi:10.1039/c8gc02800a
- Zhou R, Zhou R, Wang P, Xian Y, Mai-Prochnow A, Lu X, et al. Plasma-activated water: generation, origin of reactive species and biological applications. *J Phys D Appl Phys* (2020) 53:303001. doi:10.1088/1361-6463/ab81cf
- Gott RP, Engeling KW, Olson J, Franco C. Plasma activated water: a study of gas type, electrode material, and power supply selection and the impact on the final frontier. *Phys Chem Chem Phys* (2023) 25:5130–45. doi:10.1039/D2CP03489A
- Štěpánová V, Slavíček P, Kelar J, Prašil J, Směkal M, Stupavská M, et al. Atmospheric pressure plasma treatment of agricultural seeds of cucumber (*Cucumis sativus* L.) and pepper (*Capsicum annuum* L.) with effect on reduction of diseases and germination improvement. *Plasma Process Polym* (2018) 15. doi:10.1002/ppap.201700076
- Vichiansan N, Chatmaniwat K, Sungkorn M, Leksakul K, Chaopaisarn P, Boonyawan D. Effect of plasma-activated water generated using plasma jet on tomato (*Solanum lycopersicum* L. Var. cerasiforme) seedling growth. *J Plant Growth Regul* (2023) 42:935–45. doi:10.1007/s00344-022-10603-7
- Kučerová K, Henselová M, Slováková L, Hensel K. Effects of plasma activated water on wheat: germination, growth parameters, photosynthetic pigments, soluble protein content, and antioxidant enzymes activity. *Plasma Process Polym* (2019) 16. doi:10.1002/ppap.201800131
- Adhikari B, Adhikari M, Ghimire B, Park G, Choi EH. Cold atmospheric plasma-activated water irrigation induces defense hormone and gene expression in tomato seedlings. *Sci Rep* (2019) 9:16080. doi:10.1038/s41598-019-52646-z
- Zambon Y, Contaldo N, Laurita R, Várallyay E, Canel A, Gherardi M, et al. Plasma activated water triggers plant defence responses. *Sci Rep* (2020) 10:19211. doi:10.1038/s41598-020-76247-3
- MedCalc Software Ltd. Digimizer image analysis software ver 6.3.0 (2023). Available at: <https://www.digimizer.com/> (Accessed February 28, 2024).
- Lichtenthaler HK, Chlorophylls and carotenoids: pigments of photosynthetic biomembranes. In: *Methods in enzymology*. Academic Press (1987). p. 350–82. doi:10.1016/0076-6879(87)48036-1
- Zhang J, Kirkham MB. Antioxidant responses to drought in sunflower and sorghum seedlings. *New Phytol* (1996) 132:361–73. doi:10.1111/j.1469-8137.1996.tb01856.x
- Gambino G, Perrone I, Gribaudo I. A Rapid and effective method for RNA extraction from different tissues of grapevine and other woody plants. *Phytochem Anal* (2008) 19:520–5. doi:10.1002/pca.1078
- Abo-Zaid GA, Matar SM, Abdelhalek A. Induction of plant resistance against tobacco mosaic virus using the biocontrol agent streptomyces cellulosa isolate actino 48. *Agronomy* (2020) 10:1620. doi:10.3390/agronomy10111620
- Molinari S, Fanelli E, Leonetti P. Expression of tomato salicylic acid (SA)-responsive pathogenesis-related genes in *Mi-1*-mediated and SA-induced resistance to root-knot nematodes. *Mol Plant Pathol* (2014) 15:255–64. doi:10.1111/mpp.12085
- Song Y, Chen D, Lu K, Sun Z, Zeng R. Enhanced tomato disease resistance primed by arbuscular mycorrhizal fungus. *Front Plant Sci* (2015) 6:786. doi:10.3389/fpls.2015.00786
- Zhang Z-P, Miao M-M, Wang C-L. Effects of ALA on photosynthesis, antioxidant enzyme activity, and gene expression, and regulation of proline accumulation in tomato seedlings under NaCl stress. *J Plant Growth Regul* (2015) 34:637–50. doi:10.1007/s00344-015-9499-4
- Fuentes A, Ortiz J, Saavedra N, Salazar LA, Meneses C, Arriagada C. Reference gene selection for quantitative real-time PCR in *Solanum lycopersicum* L. inoculated with the mycorrhizal fungus *Rhizophagus irregularis*. *Plant Physiol Biochem* (2016) 101:124–31. doi:10.1016/j.plaphy.2016.01.022
- Pfaffl MW, Tichopad A, Prgomet C, Neuvians TP. Determination of stable housekeeping genes, differentially regulated target genes and sample integrity: BestKeeper – excel-based tool using pair-wise correlations. *Biotechnol Lett* (2004) 26:509–15. doi:10.1023/B:BILE.0000019559.84305.47
- Livak KJ, Schmittgen TD. Analysis of relative gene expression data using real-time quantitative PCR and the $2^{-\Delta\Delta CT}$ method. *Methods* (2001) 25:402–8. doi:10.1006/meth.2001.1262
- Terzano R, Alfeld M, Janssens K, Vekemans B, Schoonjans T, Vincze L, et al. Spatially resolved (semi)quantitative determination of iron (Fe) in plants by means of synchrotron micro X-ray fluorescence. *Anal Bioanal Chem* (2013) 405:3341–50. doi:10.1007/s00216-013-6768-6
- Voráč J, Synek P, Procházka V, Hoder T. State-by-state emission spectra fitting for non-equilibrium plasmas: OH spectra of surface barrier discharge at argon/water interface. *J Phys D Appl Phys* (2017) 50:294002. doi:10.1088/1361-6463/aa7570
- Voráč J, Kusýn L, Synek P. Deducing rotational quantum-state distributions from overlapping molecular spectra. *Rev Scientific Instr* (2019) 90:123102. doi:10.1063/1.5128455
- Voráč J, Synek P, Potočnáková L, Hnilica J, Kudrle V. Batch processing of overlapping molecular spectra as a tool for spatio-temporal diagnostics of power modulated microwave plasma jet. *Plasma Sourc Sci Technol* (2017) 26:025010. doi:10.1088/1361-6595/aa51f0
- Pei X, Gidon D, Yang YJ, Xiong Z, Graves DB. Reducing energy cost of NOx production in air plasmas. *Chem Eng J* (2019) 362:217–28. doi:10.1016/j.cej.2019.01.011
- Cherkasov N, Ibadon AO, Fitzpatrick P. A review of the existing and alternative methods for greener nitrogen fixation. *Chem Eng Process Process Intensification* (2015) 90:24–33. doi:10.1016/j.ccep.2015.02.004
- Ishibashi K, Kubota K, Kano A, Ishikawa M. Tobamoviruses: old and new threats to tomato cultivation. *J Gen Plant Pathol* (2023) 89:305–21. doi:10.1007/s10327-023-01141-5
- Porfido C, Köpke K, Allegretta I, Bandte M, von Bargen S, Rybak M, et al. Combining micro- and portable-XRF as a tool for fast identification of virus infections in plants: the case study of ASA-Virus in *Fraxinus ornus* L. *Talanta* (2023) 262:124680. doi:10.1016/j.talanta.2023.124680
- Šimek M, Homola T. Plasma-assisted agriculture: history, presence, and prospects—a review. *Eur Phys J D* (2021) 75:210. doi:10.1140/epjd/s10053-021-00206-4
- Lukes P, Dolezalova E, Sisrova I, Clupek M. Aqueous-phase chemistry and bactericidal effects from an air discharge plasma in contact with water: evidence for the formation of peroxydinitrite through a pseudo-second-order post-discharge reaction of H₂O₂ and HNO₂. *Plasma Sourc Sci Technol* (2014) 23:015019. doi:10.1088/0963-0252/23/1/015019
- Taiz L, Zeiger E. *Plant physiology*. San Francisco: Benjamin/Cummings Publishing Company (2015).
- Lamichhane P, Paneru R, Nguyen LN, Lim JS, Bhartiya P, Adhikari BC, et al. Plasma-assisted nitrogen fixation in water with various metals. *React Chem Eng* (2020) 5:2053–7. doi:10.1039/d0re00248h
- Lamichhane P, Veerana M, Lim JS, Mumtaz S, Shrestha B, Kaushik NK, et al. Low-temperature plasma-assisted nitrogen fixation for corn plant growth and development. *Int J Mol Sci* (2021) 22:5360. doi:10.3390/ijms22105360
- Busch A, Hippler M. The structure and function of eukaryotic photosystem I. *Biochim Biophys Acta (Bba) - Bioenerg* (2011) 1807:864–77. doi:10.1016/j.bbabi.2010.09.009
- Paciolla C, Fortunato S, Dipierro N, Paradiso A, De Leonardi S, Mastropasqua L, et al. Vitamin C in plants: from functions to biofortification. *Antioxidants* (2019) 8:519. doi:10.3390/antiox8110519
- Ivanov BN. Role of ascorbic acid in photosynthesis. *Biochemistry (Moscow)* (2014) 79:282–9. doi:10.1134/S0006297914030146
- Barth C, Moeder W, Klessig DF, Conklin PL. The timing of senescence and response to pathogens is altered in the ascorbate-deficient arabidopsis mutant *vitamin c-1*. *Plant Physiol* (2004) 134:1784–92. doi:10.1104/pp.103.032185
- Kacharava N, Chanishvili S, Badridze G, Chkhubianishvili E, Janukashvili N. Effect of seed irradiation on the content of antioxidants in leaves of Kidney bean. *Cabbage and Beet cultivars* (2009) 137. Available at: https://www.cropl.com/gulnara_3_3_137_145.pdf.
- Foyer CH, Noctor G. Ascorbate and glutathione: the heart of the redox hub. *Plant Physiol* (2011) 155:2–18. doi:10.1104/pp.110.167569
- Foyer CH, Kunert K. The ascorbate–glutathione cycle coming of age. *J Exp Bot* (2024):erae023. doi:10.1093/jxb/erae023
- Foyer CH, Noctor G. Redox homeostasis and antioxidant signaling: a metabolic interface between stress perception and physiological responses. *Plant Cell* (2005) 17:1866–75. doi:10.1105/tpc.105.033589
- Noctor G, Foyer CH. ASCORBATE and glutathione: keeping active oxygen under control. *Annu Rev Plant Physiol Plant Mol Biol* (1998) 49:249–79. doi:10.1146/annurev.arplant.49.1.249
- Höller S, Ueda Y, Wu L, Wang Y, Hajirezaei M-R, Ghaffari M-R, et al. Ascorbate biosynthesis and its involvement in stress tolerance and plant

- development in rice (*Oryza sativa* L.). *Plant Mol Biol* (2015) 88:545–60. doi:10.1007/s11103-015-0341-y
47. Sabetta W, Paradiso A, Paciolla C, de Pinto MC. Chemistry, biosynthesis, and antioxidative function of glutathione in plants. In: *Glutathione in plant growth, development, and stress tolerance*. Cham: Springer International Publishing (2017). p. 1–27. doi:10.1007/978-3-319-66682-2_1
48. Glazebrook J. Contrasting mechanisms of defense against biotrophic and necrotrophic pathogens. *Annu Rev Phytopathol* (2005) 43:205–27. doi:10.1146/annurev.phyto.43.040204.135923
49. Conrath U, Chapter 9 priming of induced plant defense responses. *Adv Bot Res* (2009) 51:361–95. doi:10.1016/S0065-2296(09)51009-9
50. Del Buono D, Terzano R, Panfilì I, Bartucca ML, Phytoremediation and detoxification of xenobiotics in plants: herbicide-safeners as a tool to improve plant efficiency in the remediation of polluted environments. A mini-review. *Int J Phytoremediation* (2020) 22:789–803. doi:10.1080/15226514.2019.1710817
51. Perez SM, Biondi E, Laurita R, Proto M, Sarti F, Gherardi M, et al. Plasma activated water as resistance inducer against bacterial leaf spot of tomato. *PLoS One* (2019) 14:e0217788. doi:10.1371/journal.pone.0217788